Modeling concentration polarization and fouling layers in cross-flow ultrafiltration

Gun Woo Park and Gerhard Nägele

(g.park@fz-juelich.de)

Institute of Biological Information Processing (IBI-4)

Forschungszentrum Jülich

25th ICTAM 2020+1, Milano (Virtual), Italy

SFB 985

SFB985: Functional microgel and microgel system

JÜLICH Forschungszentrum

Mitglied der Helmholtz-Gemeinschaft

Cross-flow filtration

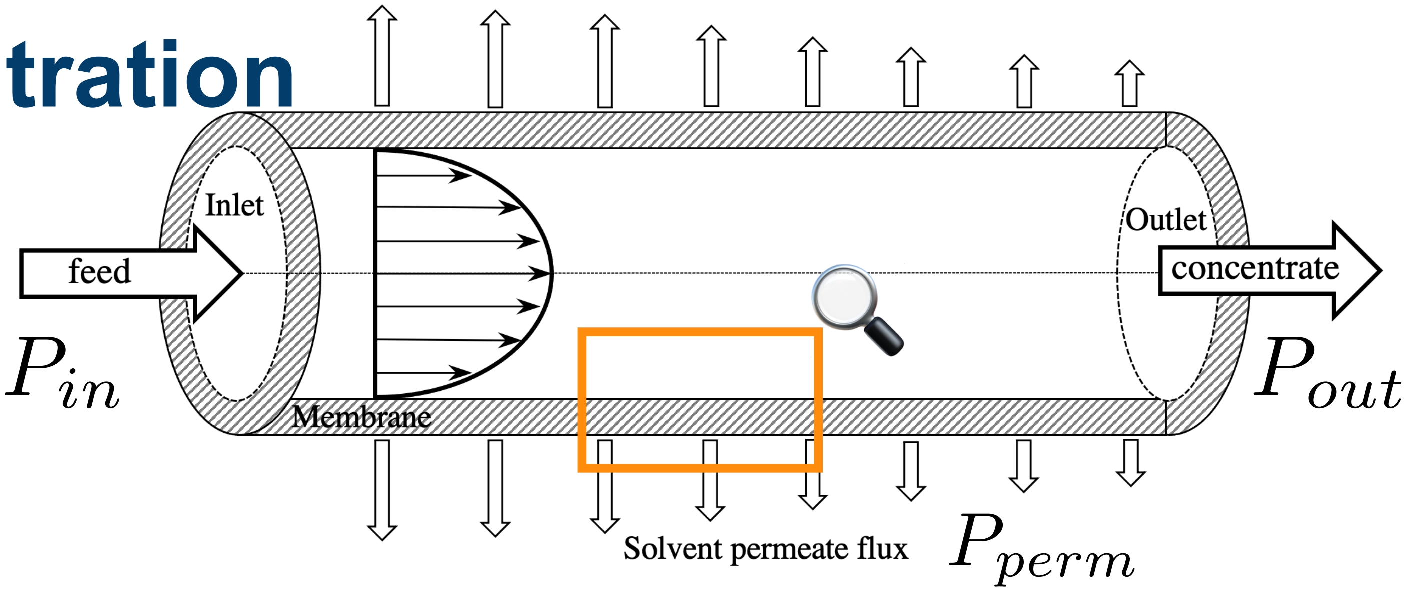

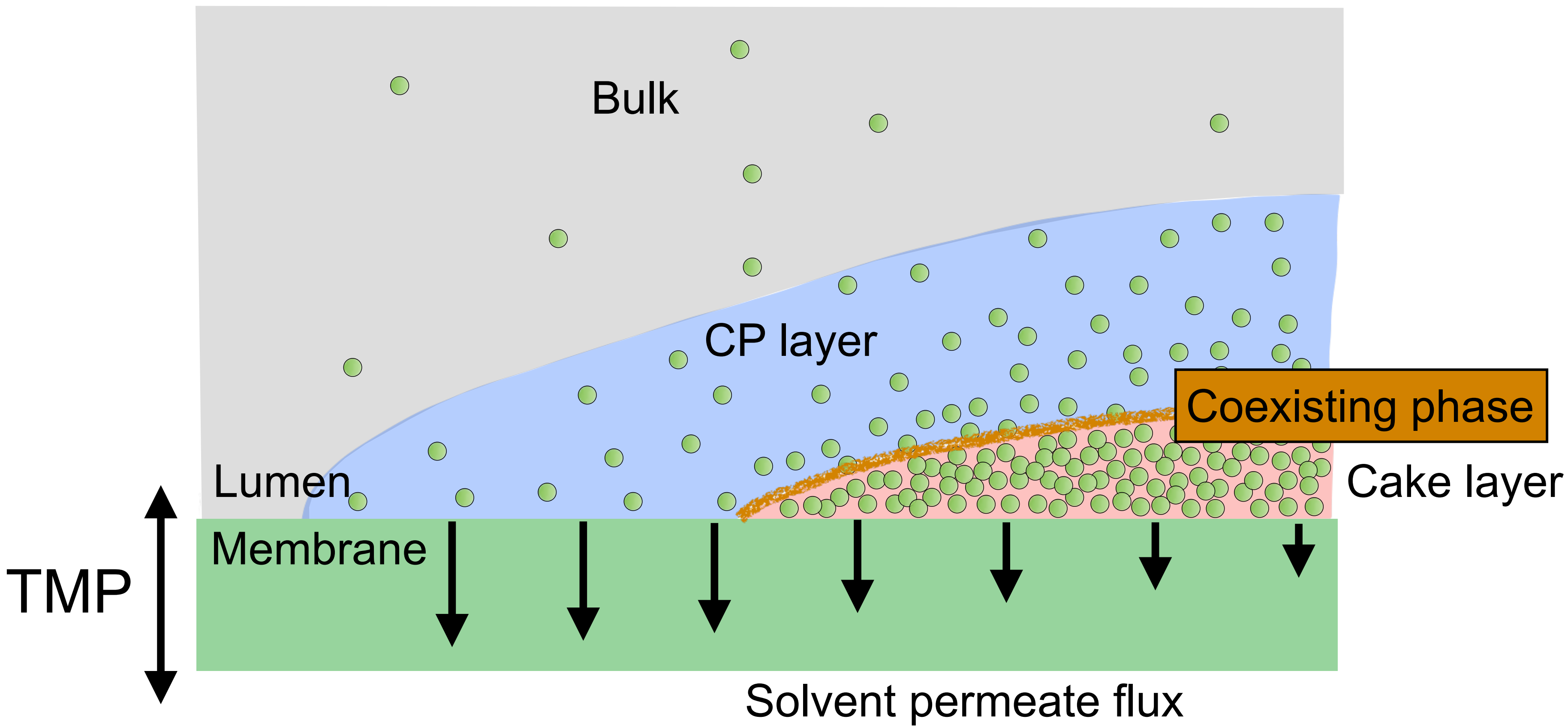

Filtration

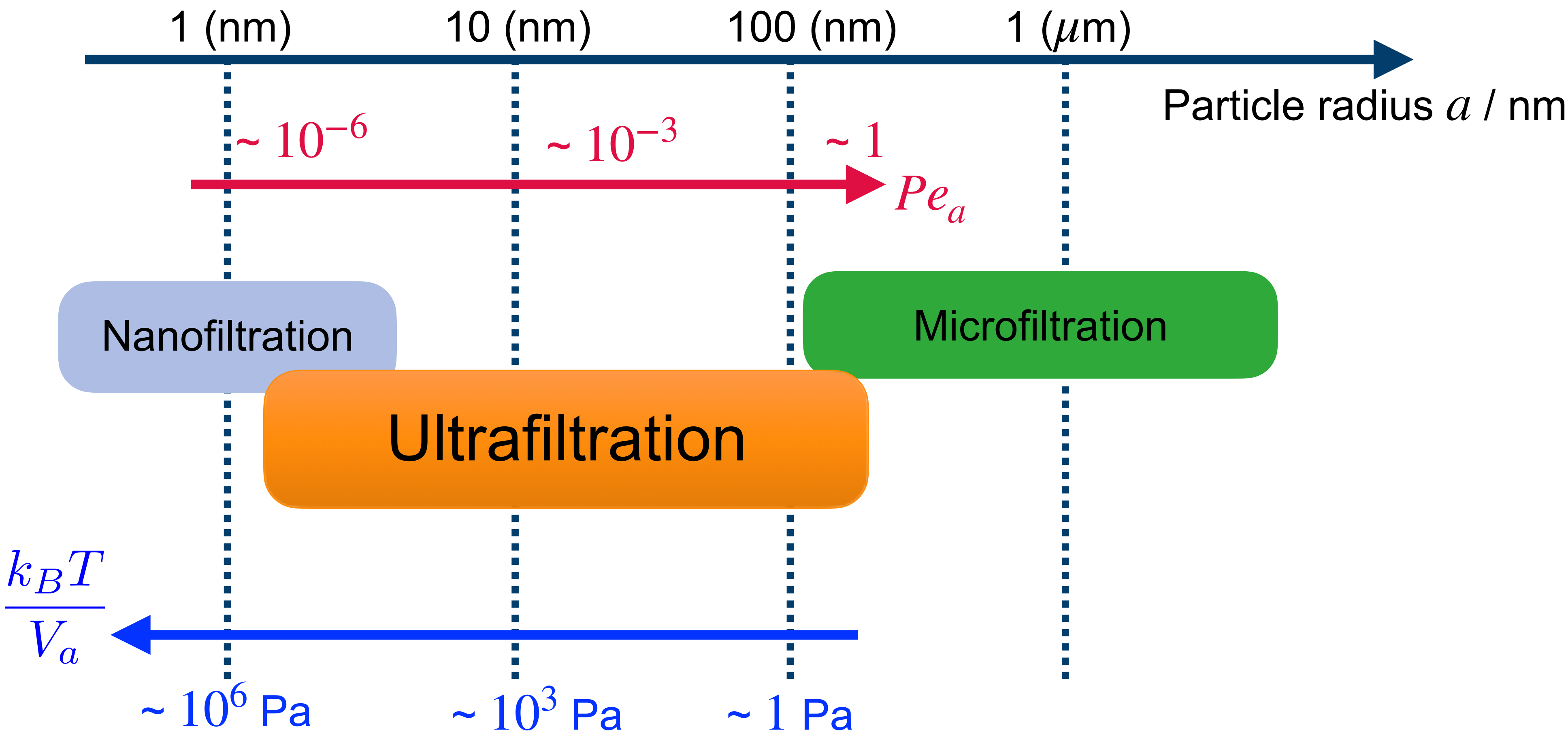

$$\Pi = \frac{k_B T}{V_a} \phi Z(\phi)$$

Particle-contributed osmotic pressure

$$Pe_a = \frac{\dot{\gamma}^* a^2}{D_0} < 1$$

Single-particle shear-Pèclet number

Steady-state flux vs TMP

Averaged Darcy-Starling equation: $\overline{v}_w = L_P \left[TMP - \overline{\Pi} \right]$

Hydraulic permeability of membrane + fouling layers

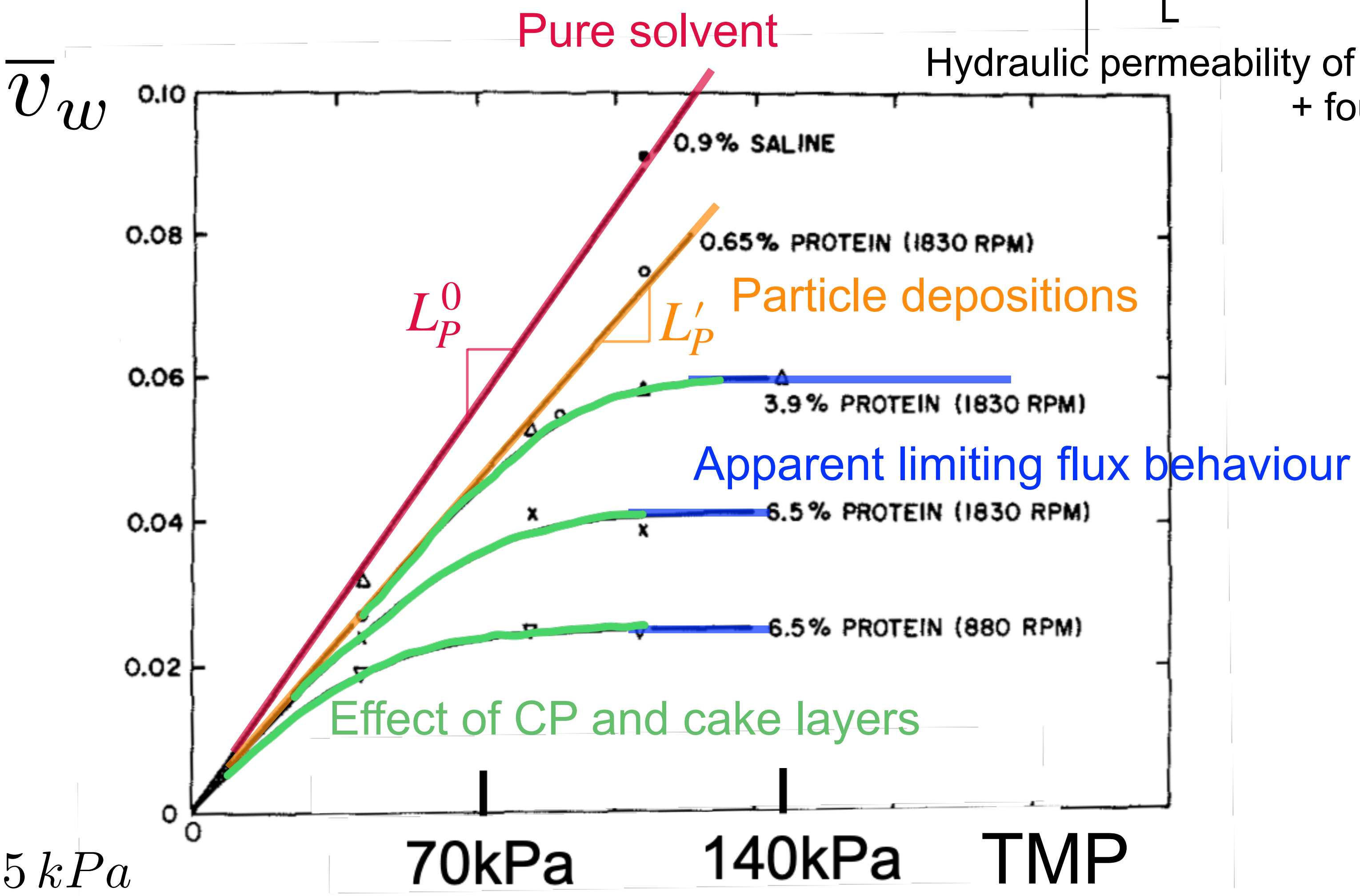

$\frac{k_B T}{V_a} \approx 35\, kPa$

(stirred-batch cell) Ultrafiltration of BSA protein solution (Blatt et al. (1970))

Critical flux and flux paradox

Critical flux = the flux at the maximum TMP before cake is formed

Bacchin et al. JMS (2006)

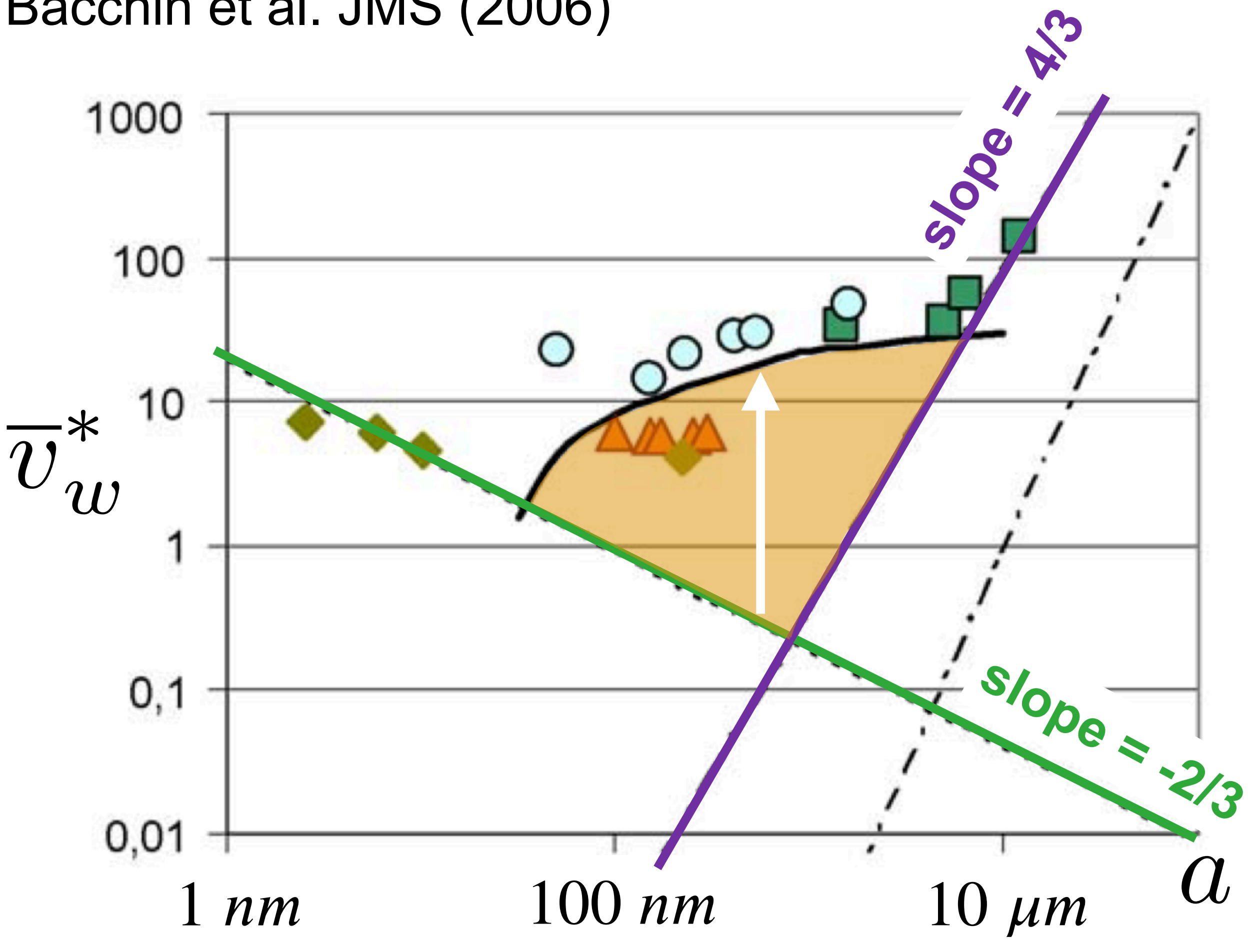

Belfort et al. JMS (1994)

Film+Gel layer model:

$$\overline{v}_w^* = K \ln \frac{\phi_f}{\phi_b}$$

Mass transfer coefficient (K):

$$K = 0.81 \left(\frac{\dot{\gamma} D^2}{L} \right)^{1/3}$$

Effective diffusion coefficient $D = ?$

1. Stokes-Einstein diffusion coefficient

$$D = D_0 = \frac{k_B T}{6\pi\eta a} \Rightarrow \overline{v}_w^* \propto a^{-2/3}$$

2. Shear-induced self-diffusion coefficient

$$D = D_S = C\,\dot{\gamma} a^2 \Rightarrow \overline{v}_w^* \propto a^{4/3}$$

(Eckstein et al. JFM 1977; Leighton and Acrivos JFM 1987)

Cross-flow ultrafiltration model

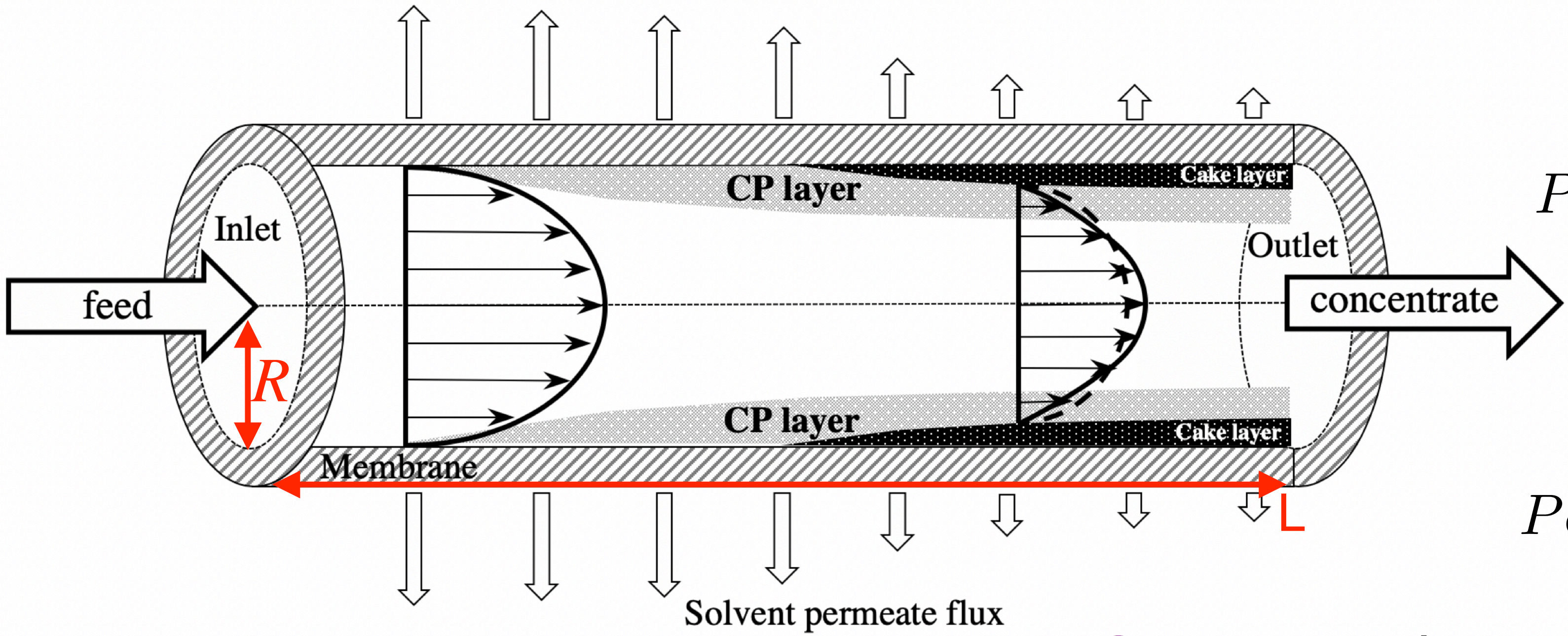

$$Re_a \ll 1$$
$$Pe_a = \frac{\dot{\gamma}^* a^2}{D_0} < 1$$
$$R/L \ll 1$$
$$Re_R \, R/L \ll 1$$
$$Pe_R = \frac{R\overline{v}_w}{D_0} \gg 1$$

UF model

Effective Stokes equation $(\mathbf{v}, P)$

Advection-diffusion equation (ϕ)

Darcy-Starling equation (v_w)

Suspension / membrane properties

- Gradient diffusion coefficient: $D(\phi)$
- Suspension viscosity: $\eta(\phi)$
- Osmotic pressure: $\Pi(\phi)$
- Hydraulic permeability: L_P^0

➡ Semi-analytic matched asymptotic solution

For details, see Park and Nägele, JCP (2020)

Neutral Brownian particles

hard spheres (**HS**)

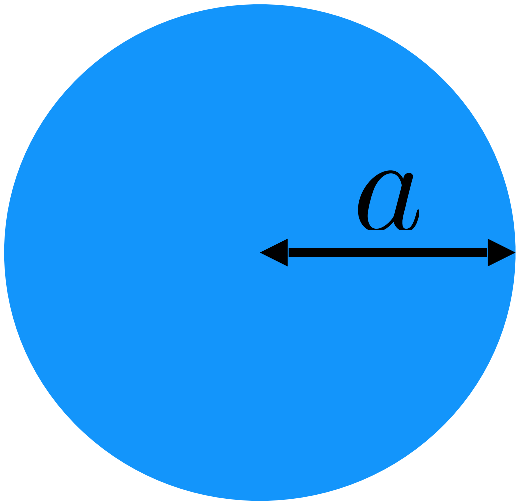

solvent-permeable
hard spheres (**PHS**)

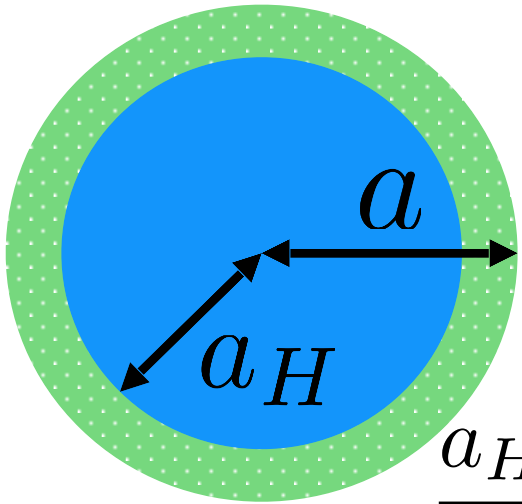

$$\Pi(\phi) = \Pi^{CS}(\phi)$$

$$D(\phi) \approx D_0 \frac{K(\phi)}{S(\phi)}$$

$$\eta(\phi)$$

$$a = 10,\ 23.82,\ 100\ (\mathrm{nm})$$

$$\frac{a_H}{a} = 0.9$$

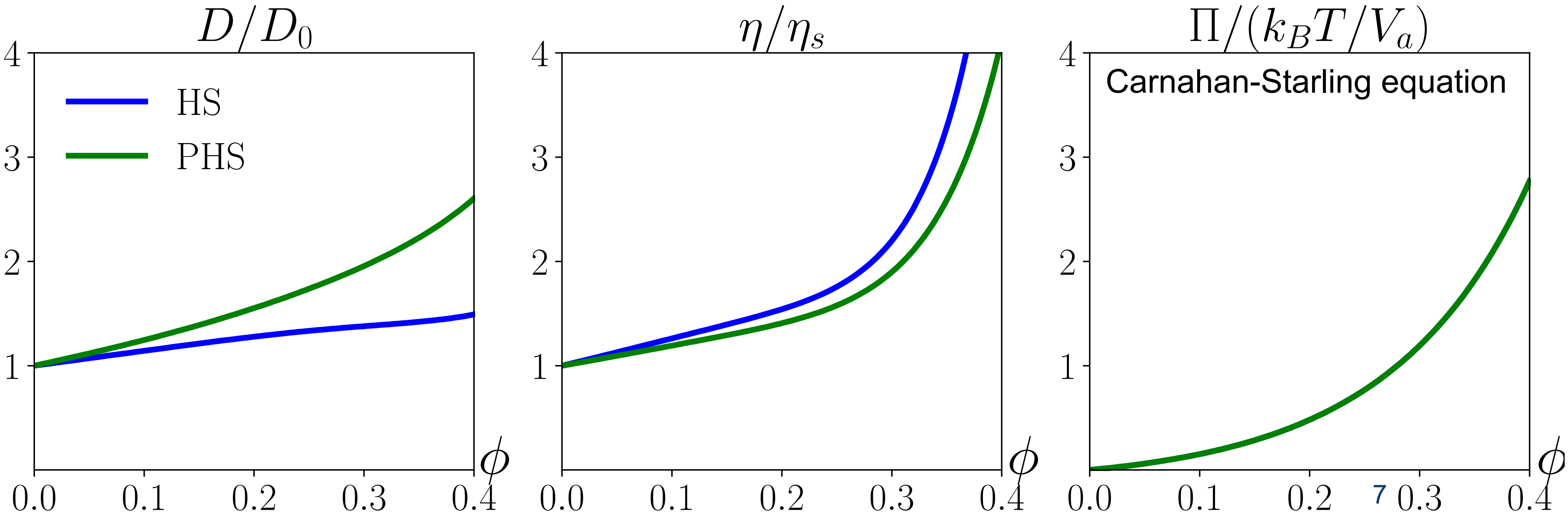

Charge-stabilized hard spheres

One-component macroion fluid model

$$\Phi \propto Z_{eff}^2 \frac{\exp(-\kappa_{eff}\, r)}{r} \quad \text{for } r > 2a$$

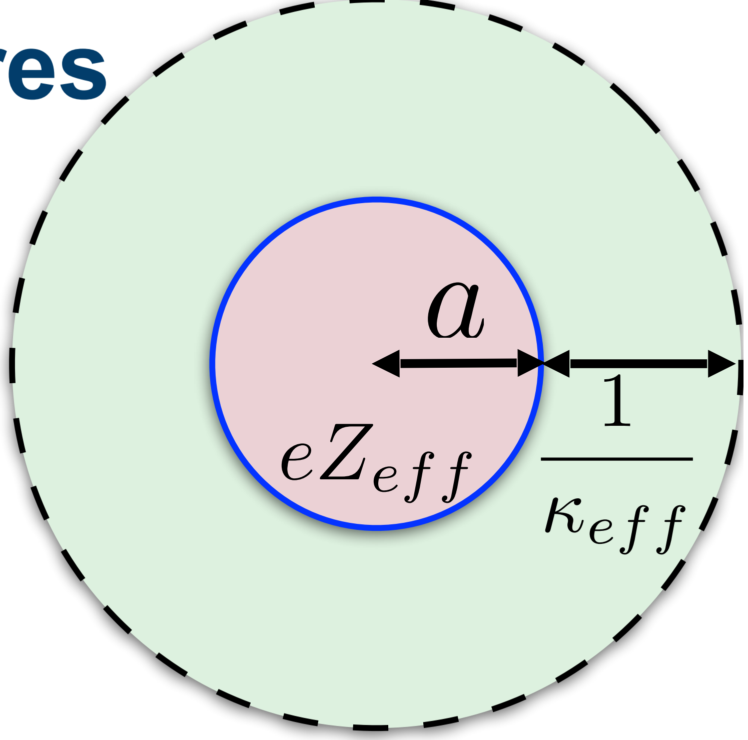

1. Determine Z_{bare} and κ for each size of particle
   (–) Z_{bare} using constant surface charge density
   (- -) Z_{bare} using constant surface potential
2. Poisson-Boltzmann cell model $Z_{bare}, \kappa \Rightarrow Z_{eff}, \kappa_{eff}$
3. Ornstein-Zernike integral theory $\Rightarrow g(r), S(q), \Pi$
4. Hydrodynamic mean-field theory $\Rightarrow D, \eta$

(Hansen-Verlet criterion of value 3.1 $\Rightarrow \phi_f$)

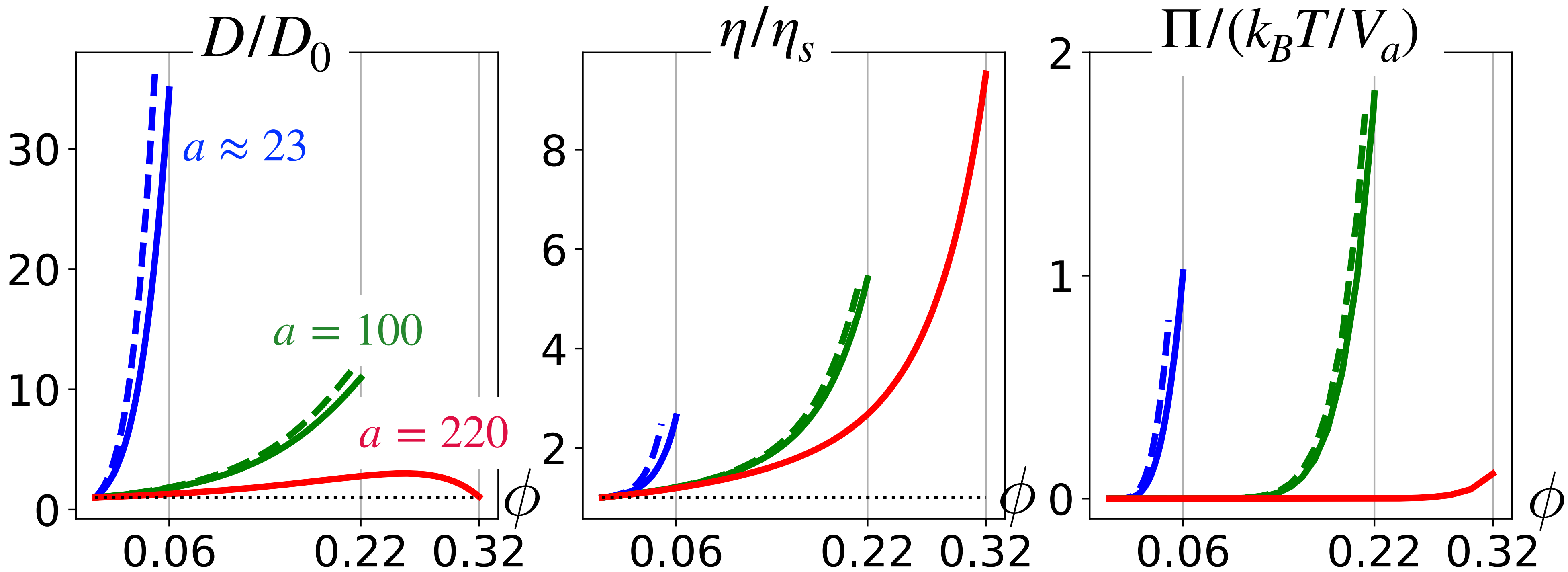

Park and Nägele, JCP, 2020

Result of CP-layer profile

(HS: a=10 nm, TMP=5 kPa)

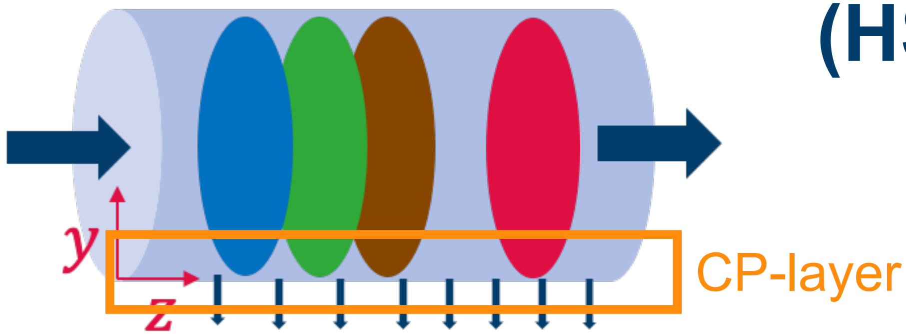

Particle concentration at wall

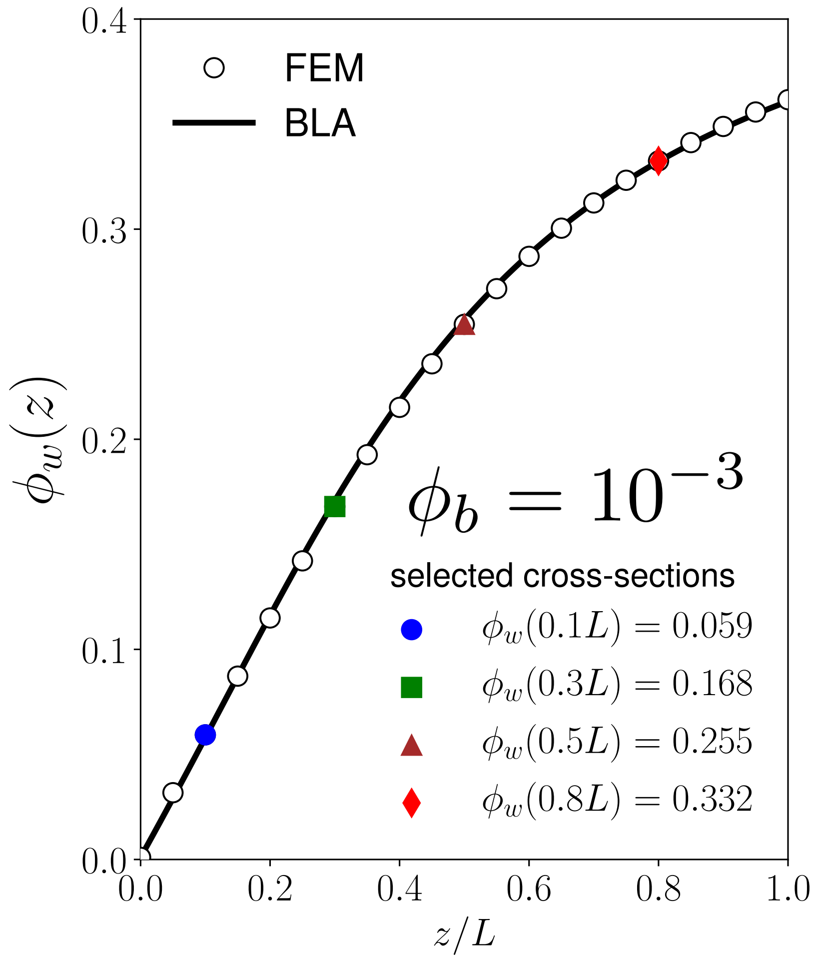

Radial particle distribution function

$$\psi(y,z) = \frac{\phi(y,z) - \phi_b}{\phi_w(z) - \phi_b}$$

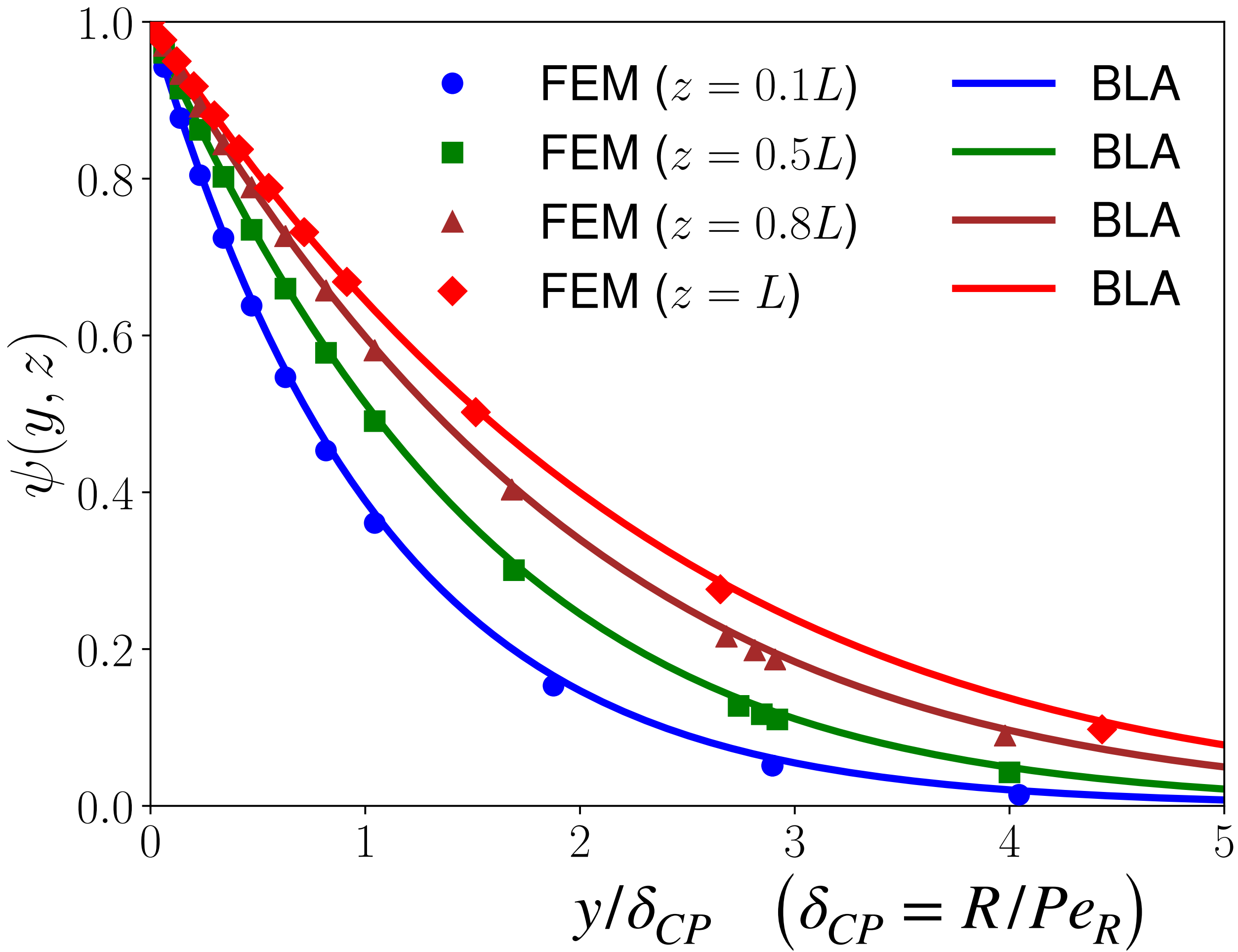

Effect of CP and Cake layers (a=10nm)

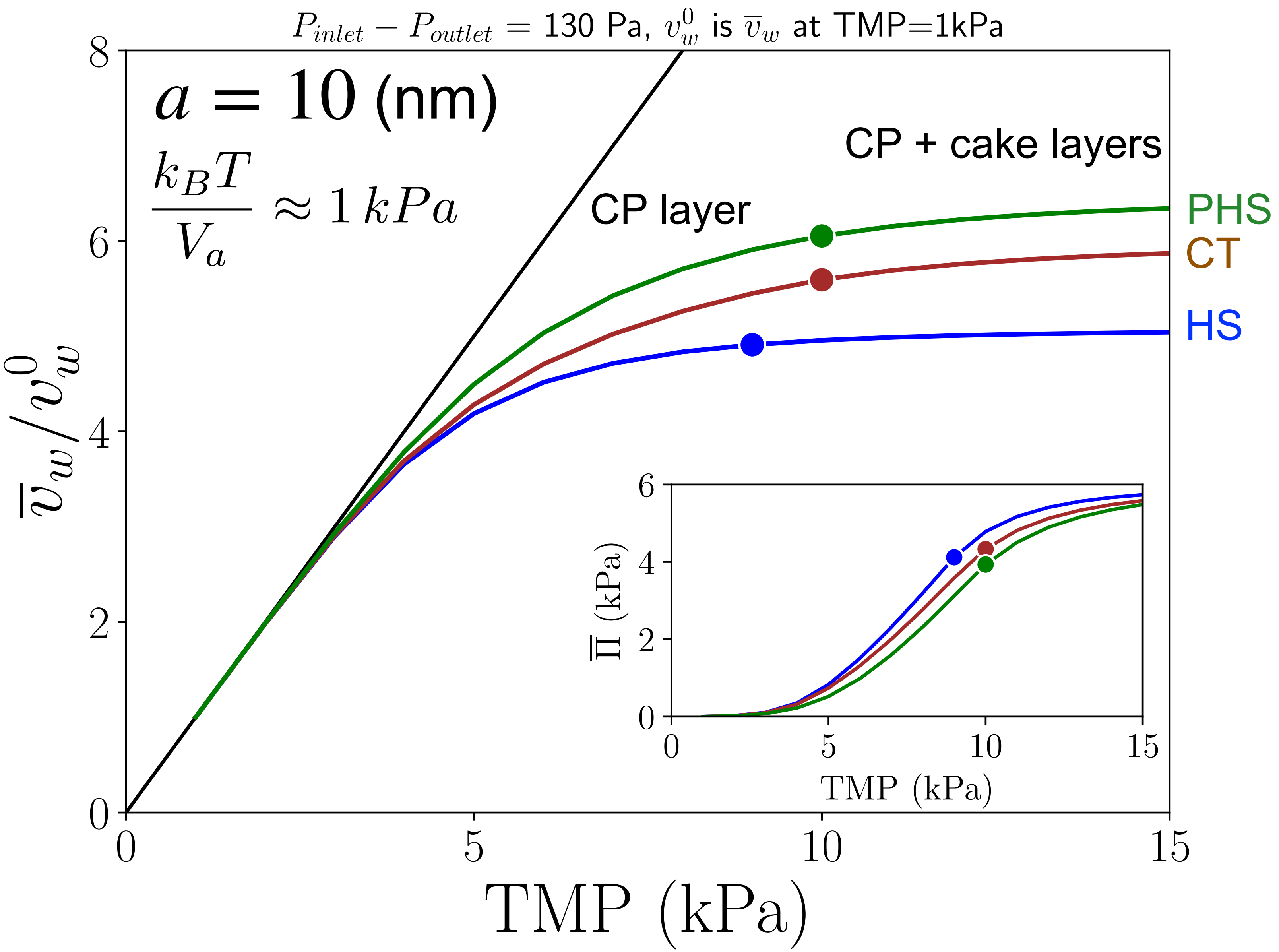

Park and Nägele, to be submitted (2021)

Various particle systems ($a \approx 23$nm)

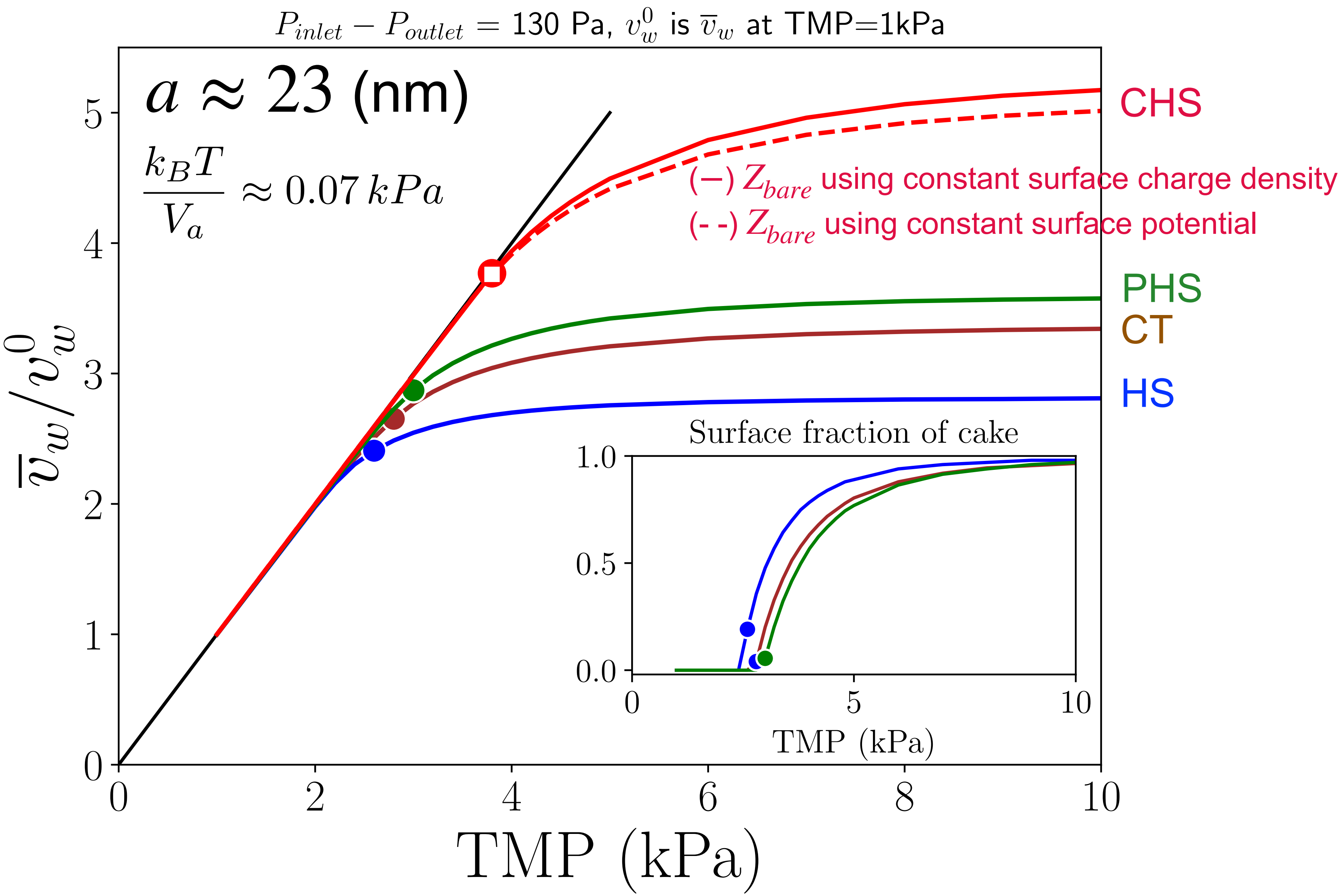

Park and Nägele, to be submitted (2021)

Critical flux vs. particle radius a

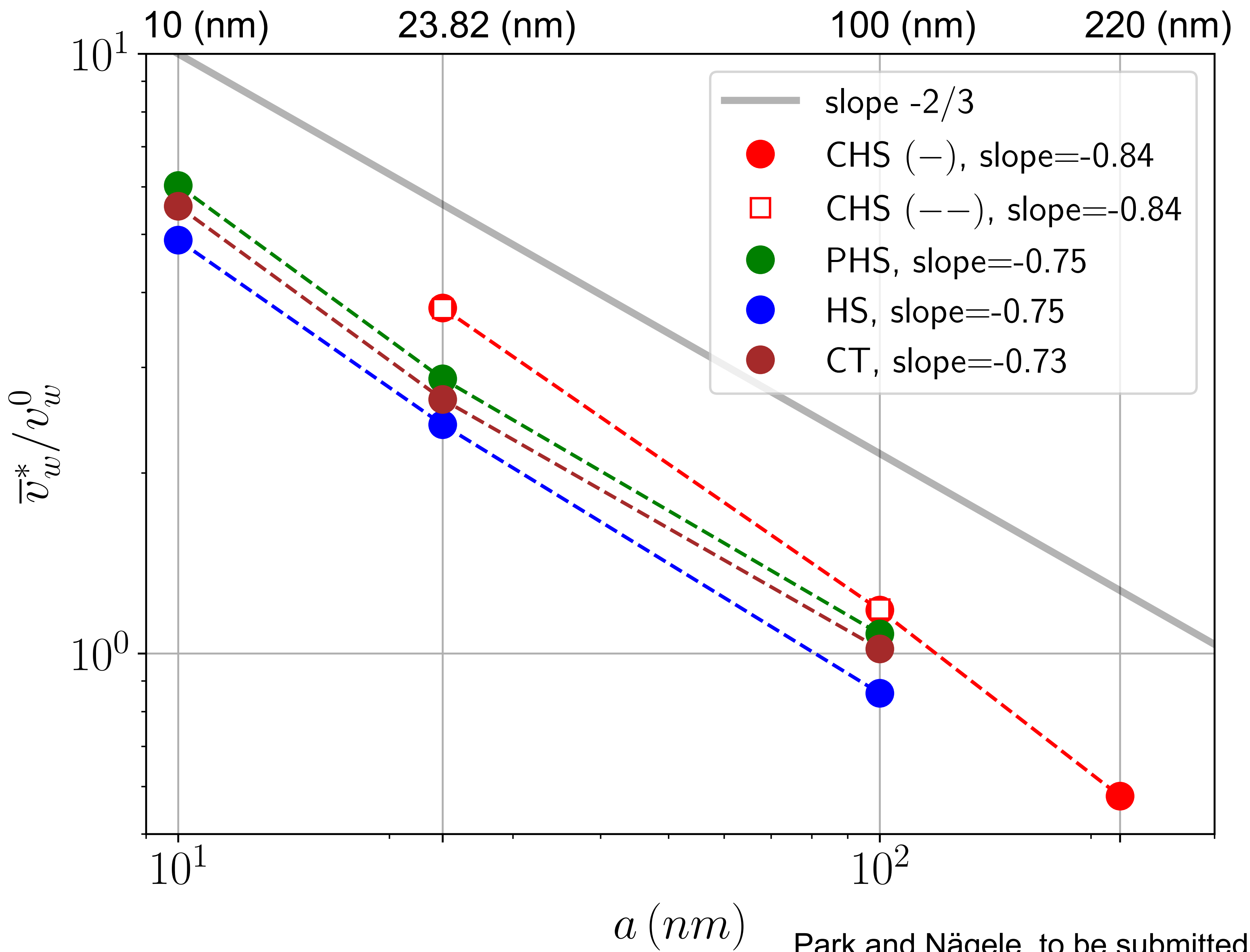

Park and Nägele, to be submitted (2021)

Summary

1. Describe recent boundary layer analysis for cross-flow ultrafiltration (Park and Nägele, JCP, 2020) with a simplified cake layer model.
2. Suspension properties discussed for neutral Brownian hard spheres (HS), neutral solvent-permeable hard spheres (PHS), and charged hard spheres (CHS).
3. Effect of CP-layer on permeate flux strongly depends on size of particles. For larger particles (> 10nm), cake formation is dominant factor for reduction of permeate flux.
4. Critical and apparent limiting flux concepts are introduced, and applied to current model. Both charged and neutral particle systems show similar power-low behavior for critical flux vs. particle size.
5. This indicates that mechanisms not considered in our model may be responsible for flux paradox, e.g.: pore clogging, adsorption layer, and shear-induced migration.

Thank you

Institute of Biological Information Processing (IBI-4), Forschungszentrum Jülich

SFB
985

SFB985: Functional microgel and microgel system

JÜLICH
Forschungszentrum

Mitglied der Helmholtz-Gemeinschaft